The Crystal Structure of Tetrabutylammonium Tetrakis(4,4,4-trifluoro-1-(2-thienyl)-1,3-butanedione)praseodymium(III), $(C_4H_9)_4N(C_8H_4F_3O_2S)_4Pr(III)$

RONALD T. CRIASIA

Chemistry–Physics Department, Kean College of New Jersey, Union, N.J. 07083, U.S.A.

(Received March 23, 1987)

Abstract

The crystal structure of tetrabutylammonium tetrakis(4,4,4-trifluoro-1-(2-thienyl)-1,3-butanedione praseodymium(III), $(C_4H_9)_4N(C_8H_4F_3O_2S)_4Pr(III)$, has been determined using 2300 independent, visually estimated intensities and refined by full matrix least-squares methods to $R = 0.118$, $R_w = 0.149$. The crystals are monoclinic with $a = 22.32(5)$, $b = 10.45(2)$, $c = 12.23(3)$ Å, $\beta = 96.7(4)°$. The space group is $P2/n$ with $Z = 2$, requiring a 2-fold axis in both the anion and cation. The coordination sphere has an arrangement close to that of a square antiprism but with small distortions in the direction of a dodecahedron. Pr–O bond distances range from 2.42–2.47 Å.

Introduction

The tetrakis chelates TBA Ln(TTA)$_4$ (where TBA = tetrabutylammonium and HTTA = 4,4,4-trifluoro-1-(2-thienyl)-1,3-butanedione) were prepared for all lanthanides except promethium [1]. It was found that the crystals of the whole series form only two isomorphs. The crystal structure of an example of one isomorph, that of the samarium compound, has been described in an accompanying paper [2], and details of the structure of the praseodymium compound, as typical of the other isomorph, are presented here.

Experimental

Preparations

The compound was prepared, and crystals grown as described previously [1]. *Anal.* Found: C, 45.40; H, 4.47; N, 1.26; Pr, 10.99. Calc. C, 45.32; H, 4.44; N, 1.10%; S, 10.08; Pr, 11.08%.

X-ray Study

One of the clear, green crystals was selected for data collection. From Weissenberg and precession photographs the crystals were found to be monoclinic, space group *Pn* or *P2/n*, with cell constants $a = 22.32(5)$*, $b = 10.45(2)$, $c = 12.23(3)$ Å, $\beta = 96.7(4)°$, $Z = 2$, $D_{calc} = 1.49$, $D_{obs} = 1.47$ g cm^{-3} by flotation in carbon tetrachloride–ethylbenzene solution at 25 °C). Intensity data were collected for the reciprocal lattice levels *h0l–h8l* by the equi-inclination Weissenberg method using the multiple film technique with Ni-filtered Cu Kα radiation, and for the *hk*0 and 0*kl* zones on precession photographs with Zr-filtered Mo Kα radiation. The intensities of 2300 independent reflections were estimated visually by comparison with a time-calibrated intensity scale. The precession photographs were used for the initial scaling of the different Weissenberg levels, although this later proved unsatisfactory. A set of F_os was derived by application of Lorentz-polarization and spot distortion factors [3, 4]. Unfortunately the crystal, which was elongated along the *b*-axis, was accidentally destroyed before accurate dimensional measurements could be made, and absorption corrections could not therefore be applied. Since μ for Cu Kα is 81.2 cm^{-1}, absorption is undoubtedly a source of error in the final results, and the e.s.d.'s given must be regarded as minimal.

Structure Determination and Refinement

The Patterson map had its largest peak (Pr–Pr vector) on the line 1/2, *v*, 1/2, suggesting that the Pr atoms lay on two-fold axes in the space group *P2/n***. Accordingly, structure determination and refinement were carried out in the centrosymmetric space group and this assignment seems justified by the results. All other non-hydrogen atoms in the molecule were located from successive electron density maps using initial phases calculated from the Pr positions.

Refinement was carried out by full matrix least squares methods. At a late stage separate scale factors for the different Weissenberg levels were refined. On refining anisotropic thermal parameters for all atoms

---

*Here, and throughout this paper, estimated standard deviations, shown in parentheses, are right-adjusted to the least significant digit in the preceding number.

**The non-standard setting used has coordinates of equivalent positions: $\pm(x, y, z; \frac{1}{2} - x, y, \frac{1}{2} - z)$.

0020-1693/87/$3.50

TABLE I. Fractional Coordinates for all Atoms ($\times 10^4$), Anisotropic Thermal Parameters[a] for Pr ($\times 10^4$) and Isotropic Thermal Parameters for the other Atoms

Atom	x	y	z	β_{11}	β_{22}	β_{33}	β_{12}	β_{13}	β_{23}
Pr	2500(0)	245(1)	2500(0)	7(0)	26(6)	51(1)	0(0)	4(0)	0(0)

Atom	x	y	z	B (Å^2)
O(1)	1489(4)	927(8)	1731(7)	7.7(2)
O(2)	1963(4)	−1462(9)	1464(7)	8.4(2)
F(1)	389(9)	1853(19)	533(16)	9.0(5)
F(2)	511(9)	2076(19)	2238(15)	8.2(4)
F(3)	−54(15)	460(28)	1514(26)	12.9(8)
C(1)	469(10)	1094(21)	1560(17)	3.8(4)
C(2)	991(7)	375(17)	1571(14)	2.4(3)
C(3)	923(11)	−969(23)	1399(20)	4.4(5)
C(4)	1391(7)	−1811(17)	1335(14)	2.4(3)
C(5)	1303(9)	−3111(21)	1227(16)	3.5(4)
C(6)	693(9)	−3812(21)	1036(17)	3.7(4)
C(7)	840(20)	−5095(38)	992(36)	8.2(10)
C(8)	1419(20)	−5427(39)	1135(34)	8.5(9)
S(1)	1889(4)	−4176(8)	1250(7)	6.6(2)
O(3)	2745(7)	1889(16)	1175(13)	4.8(3)
O(4)	3160(6)	−708(15)	1236(12)	4.0(3)
F(4)	2831(15)	3599(31)	−520(25)	13.1(8)
F(5)	3739(14)	3461(27)	−239(24)	13.5(8)
F(6)	3143(17)	4159(38)	796(30)	16.5(10)
C(9)	3235(25)	3239(51)	196(43)	8.6(12)
C(10)	3187(10)	1956(23)	607(19)	4.4(4)
C(11)	3554(13)	973(26)	310(22)	5.6(5)
C(12)	3532(9)	−228(20)	661(17)	3.6(4)
C(13)	3954(10)	−1223(22)	335(18)	4.5(4)
C(14)	4437(12)	−1051(24)	−459(20)	4.7(5)
C(15)	4761(16)	−2234(34)	−418(29)	8.9(8)
C(16)	4560(16)	−3161(35)	276(28)	7.5(8)
S(2)	3950(5)	−2666(10)	908(8)	8.3(2)
N	2500(0)	−2172(44)	−2500(0)	7.5(10)
C(17)	2380(22)	−1375(43)	−1565(35)	9.2(11)
C(18)	1868(29)	−404(54)	−1962(52)	13.6(15)
C(19)	1761(35)	393(63)	−1050(62)	14.4(20)
C(20)	1260(63)	1356(127)	−1903(114)	30.7(47)
C(21)	3048(24)	−3098(48)	−2080(41)	9.8(12)
C(22)	3361(62)	−3818(130)	−3009(108)	24.6(42)
C(23)	3856(64)	−4757(114)	−2832(118)	24.8(44)
C(24)	4248(36)	−3769(70)	−2976(54)	19.7(19)

[a] The anisotropic temperature factor used was of the form $\exp[-(\beta_{11}h^2 + \beta_{22}k^2 + \beta_{33}l^2 + 2\beta_{12}hk + 2\beta_{13}hl + 2\beta_{23}kl)]$. [b] Isotropic temperature factors used were of the form $\exp(-B\sin^2\theta/\lambda^2)$.

several of the β_{11} parameters became negative, indicating that the quality of the data was inadequate for such a model. Final refinement was therefore carried out on all positional parameters, nine scale factors, anisotropic thermal parameters for Pr and isotropic thermal parameters for all other (non-hydrogen) atoms. The function minimized was $\Sigma w(|F_o| - |F_c|)^2$ where $w = 1/\sigma^2$ for each reflection and σ was obtained from the standard deviations estimated in the original intensity measurements. Unobserved reflections were weighted zero. The final value of R was 0.118 and of R_w was 0.149. The 'error of fit' function, $[\Sigma w(|F_o| - |F_c|)^2/(n-m)]^{1/2}$, where n is the number of observations and m the number of variable parameters, was 1.40. The atomic scattering factors used for Pr was that given by Cromer and Waber [5], and for the other atoms the values given in the International Tables were used [6]. Anomalous dispersion corrections were applied for Pr and S atoms [7]. A table of the final observed and calculated values of the structure factors may be obtained from the Editor. Major computing programs used were modifications of INSCALE [8], ORFLS [9], FORDAP [10], ORFFE [11], PLANET [12] and ORTEP [13].

Results and Discussion

Fractional atomic coordinates for all atoms, anisotropic thermal parameters for Pr and isotropic parameters for the other atoms are given in Table I. A stereoview of the whole unit cell is shown in Fig. 1, where it can be seen that the structure consists of discrete TBA cations and $Pr(TTA)_4^-$ anions. The numbering scheme used, and also the bond distances and bond angles in the anion and cation are shown in Fig. 2(a) and (b), respectively.

The geometry of the anion is shown in Fig. 3, a stereoview with the Pr coordination sphere emphasized. It is clear that the coordinating oxygen atoms are arranged close to the vertices of a square antiprism, and the independent O–O distances are therefore shown in Fig. 4, which gives the idealized square antiprism geometry. More detailed examination, however, shows deviations from the ideal geometry. Some of these are due to the differentiation between equivalent vertices by the attachment of the bidentate ligands, but others appear to be systematic. The 'square' faces show small but significant deviations from planarity of up to 0.14 Å. These are in a direction of a folding about O(1)–O(4) and O(1′)–O(4), which is indicative of the creation of two new faces in the polyhedron, as required by a dodecahedron. The dihedral angle between the planes O(1)–O(2)–O(4) and O(1)–O(3)–O(4) is 10.5°. This angle would be 29.5° for a dodecahedron and 0° for a square antiprism [14]. On the other hand the average dihedral angle between adjacent triangular faces on the antiprism model is 51.0°, decreased by 6% from the ideal antiprism value of 52.4° towards that of 29.5° for the dodecahedron [14]. Another sensitive test used in the differentiation of these geometries is examination of the characteristics of the trapezoids O(1), O(2), O(2′), O(1′)

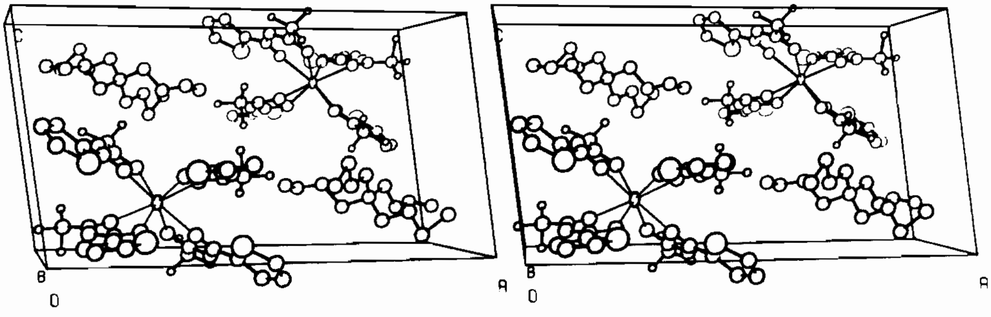

Fig. 1. A stereoview of the contents of one unit cell.

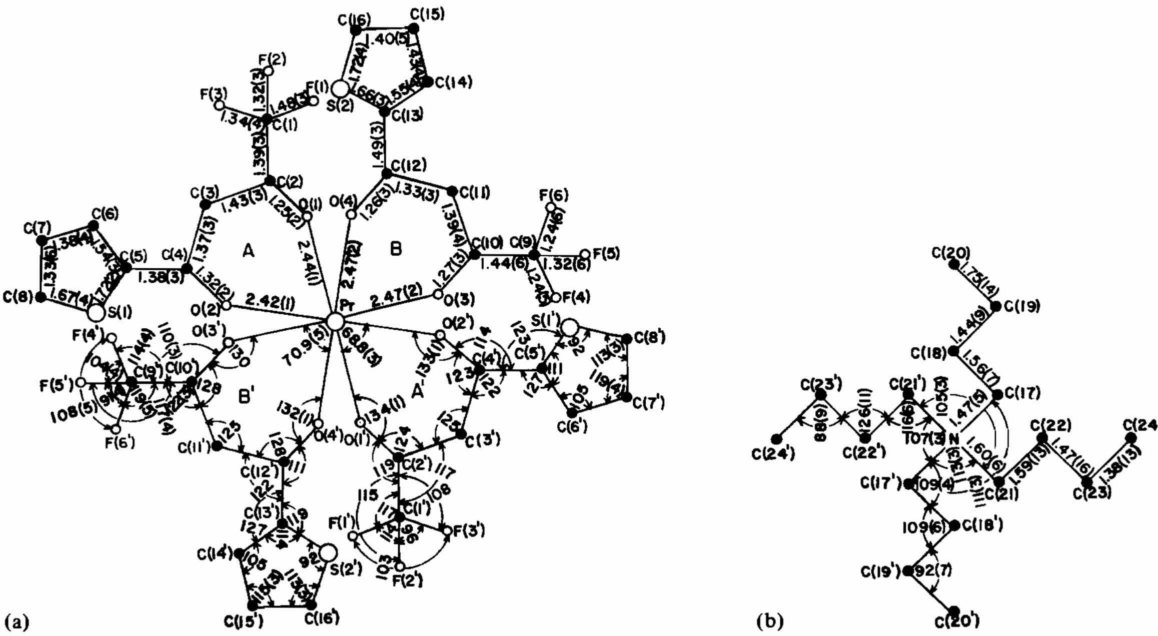

Fig. 2. The numbering scheme employed with bond distances in Å and bond angles in degrees for the anion in (a) and the cation in (b). In the anion the standard deviations of bond angles are 2° where these are not shown.

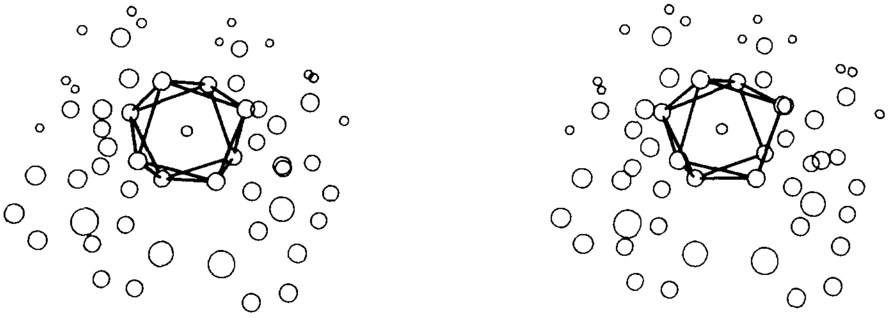

Fig. 3. A steroview of the anion with the coordination sphere polyhedron outlined.

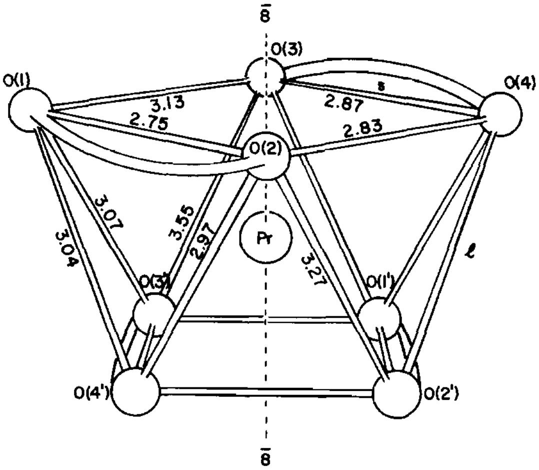

Fig. 4. An idealized square antiprism showing ligand attachment and independent distances between adjacent oxygen atoms.

and O(3), O(4), O(4′), O(3′) [15]. In the dodecahedron these are planar and orthogonal. In Pr-$(TTA)_4^-$ they are far from planar with deviations of up to 0.53 Å from the least squares mean planes, and their dihedral angle is 81.5° as compared to the ideal antiprism angle of 77.4°. Using the notation of Hoard [16], the ratio of the l to s edge lengths (Fig. 4) is 1.076 in this anion as compared to 1.057 for the most favorable antiprism geometry, while the average angle between the Pr–O bonds and the (ideal) $\bar{8}$ axis of the antiprism is 59.0° as compared to the calculated value of 57.3°. In summary, the geometry of the coordination sphere is closer to that of a square antiprism but does seem to have a small fraction of dodecahedral character. Other features of the anion geometry are similar to those noted in related structures [2, 17–19]. The chelate backbone atoms are coplanar within experimental error, but the six-membered rings formed by inclusion of the Pr atom are folded about O(1)–O(2) by 27.7° in ligand A and about O(3)–O(4) by 12.6° in ligand B. This folding appears to relieve interligand strain.

The thienyl rings are themselves coplanar but make a dihedral angle with the chelate backbone planes of 9.6° and 9.1° in ligands A and B, respectively. The thienyl rings are arranged so that there are non-bonded interactions shorter than the van der Waals' distance of 2.58 Å between S(1) and O(2) and 2.76 Å between O(4) and S(2). These close approaches are facilitated by the widening of the angles C(4)–C(5)–C(6) and C(12)–C(13)–C(14).

The Pr–O distances vary from 2.42–2.47 Å and the 'bite' of the chelate, the distance between O(1)–O(2) and O(3)–O(4), averages 2.81 Å, in good agreement with corresponding measurements in related compounds. However, outside the central part of the anion the bond distances are not accurate enough to merit serious discussion. This is particularly true in the cation as shown by the poor bond distances as compared to standard values and the high thermal parameters. The positions of C(20), the terminal atom of one butyl group, is very poorly defined and disorder may be involved in this region.

Acknowledgements

The author is indebted to Brookhaven National Laboratory for the use of their facilities and to S. J. LaPlaca, I.B.M. Corporation, T. J. Watson Research Center, Yorktown Heights, N. Y. and J. White, Fordham University, Bronx, N.Y.

References

1 R. T. Criasia and M. Cefola, *J. Inorg. Nucl. Chem.*, *37*, 1814 (1975).
2 R. T. Criasia, submitted for publication.
3 D. C. Phillips, *Acta Crystallogr.*, *7*, 746 (1954).
4 D. C. Phillips, *Acta Crystallogr.*, *9*, 812 (1956).
5 D. T. Cromer and J. T. Waber, *Acta Crystallogr.*, *18*, 104 (1965).
6 'International Tables for X-ray Crystallography', Vol. III, Kynoch Press, Birmingham, p. 202.
7 D. T. Cromer, *Acta Crystallogr.*, *18*, 17 (1965).

8 W. C. Hamilton, J. S. Rollett and R. A. Sparks, *Acta Crystallogr., 18*, 129 (1965).

9 W. R. Busing, K. O. Martin and H. A. Levy, 'ORFLS', a Fortran crystallographic least-squares program, *ORNL-TM-305*, Oak Ridge National Laboratory, Oak Ridge, Tenn., 1962.

10 A. Zalkin, 'FORDAP, a Fortran crystallographic program for Fourier analysis', University of California, Livermore, 1962.

11 W. R. Busing, H. O. Martin and H. A. Levy, 'ORFFE', a Fortran crystallographic function and error program', *ORNL-TM-306*, Oak Ridge National Laboratory, Oak Ridge, Tenn. 1962.

12 D. L. Smith, *Ph.D. Thesis*, University of Wisconsin, (1962).

13 C. K. Johnson, 'ORTEP', a Fortran thermal ellipsoid plot program for crystal structure illustrations', *ORNL-3794*, Oak Ridge National Laboratory, Oak Ridge, Tenn., 1965.

14 E. L. Muetterties and L. J. Guggenberger, *J. Am. Chem. Soc., 96*, 1748 (1974).

15 S. J. Lippard and B. J. Ross, *Inorg. Chem., 7*, 1886 (1968).

16 J. L. Hoard and J. V. Silverton, *Inorg. Chem., 2*, 235 (1963).

17 R. A. Lalancette, M. Cefola, W. C. Hamilton and S. J. LaPlaca, *Inorg. Chem., 6*, 2127 (1967).

18 J. G. White, *Inorg. Chim. Acta, 16*, 159 (1976).

19 A. T. McPhail and Pui Suen Wong Tschang, *J. Chem. Soc., Dalton Trans.*, 1165 (1974).